ACS Infectious Diseases

Article

Inhibiting the #-Lactamase of Mycobacterium tuberculosis (Mtb) with Novel Boronic-Acid-Transition-State-Inhibitors (BATSIs)

Sebastian G. Kurz, Saugata Hazra, Christopher R. Bethel, CHIARA ROMAGNOLI, Emilia Caselli, Fabio Prati, John S. Blanchard, and Robert A. Bonomo

ACS Infect. Dis., **Just Accepted Manuscript** • DOI: 10.1021/acsinfecdis.5b00003 • Publication Date (Web): 19 Mar 2015

Just Accepted

ACS Infectious Diseases is published by the American Chemical Society. 1155 Sixteenth Street N.W., Washington, DC 20036

Inhibiting the β-Lactamase of *Mycobacterium tuberculosis* (Mtb) with Novel Boronic-Acid-Transition-State-Inhibitors (BATSIs)

Sebastian G Kurz*[1], Saugata Hazra*[2], Christopher R Bethel[3], Chiara Romagnoli[4], Emilia Caselli[4], Fabio Prati[4#], John S Blanchard[5#], Robert A Bonomo[6,7,8#]

[1]Department of Medicine, Tufts Medical Center, 600 Washington St. #257, Boston, MA 02111, USA; [2]Department of Biotechnology, Indian Institute of Technology Roorkee (IITR) Roorkee, Uttarakhand 247667, India; [3]Research Service, Louis Stokes Cleveland Veterans Affairs Medical Center, 10701 East Boulevard, Cleveland, OH 44106, USA; [4]Department of Life Science, University of Modena and Reggio Emilia. Via Campi 183, 41100 Modena, Italy; [5]Department of Biochemistry, Albert Einstein College of Medicine, 1300 Morris Park Avenue, Bronx, NY 10461, USA; [6]Department of Biology and Microbiology and [7]Department of Pharmacology, Case Western Reserve University School of Medicine, Cleveland, OH 44106, USA; [8]Department of Medicine, Louis Stokes Cleveland Veterans Affairs Medical Center, 10701 East Boulevard, Cleveland, OH 44106, USA

*Both authors contributed equally to the manuscript

#corresponding author: fabio.prati@unimore.it; john.blanchard@einstein.yu.edu; robert.bonomo@va.gov;

BlaC, the single chromosomally-encoded β-lactamase of *Mycobacterium tuberculosis,* has been identified as a promising target for novel therapies that rely upon β-lactamase inhibition. Boronic acid transition state inhibitors (BATSIs) are a class of β-lactamase inhibitors which permit rational inhibitor design by combinations of various R1 and R2 side chains. To explore the structural determinants of effective inhibition, we screened a panel of 25 BATSIs to explore key structure-function relationships. We identified a cefoperazone analogue, EC19, which displayed slow, time-dependent inhibition against BlaC with a potency similar to clavulanate. To further characterize the molecular basis of inhibition, we solved the three-dimensional structure of the EC19-BlaC complex and expanded our analysis to variant enzymes. The results of this structure-function analysis encourage the design of a novel class of β-lactamase inhibitors, BATSIs, to be used against *Mycobacterium tuberculosis.*

Key words:
Mycobacterium tuberculosis
Beta-lactamase inhibition
Boronic-Acid-Transitional-State-Inhibitors
Acylation high-energy intermediate
Deacylation high-energy intermediate
Cefoperazone Analogue EC19

For Table of Contents Use Only: Inhibiting the β-Lactamase of Mycobacterium tuberculosis (Mtb) with Novel Boronic-Acid-Transition-State-Inhibitors (BATSIs)

Sebastian G Kurz, Saugata Hazra, Christopher R Bethel, Chiara Romagnoli, Emilia Caselli, Fabio Prati, John S Blanchard, Robert A Bonomo

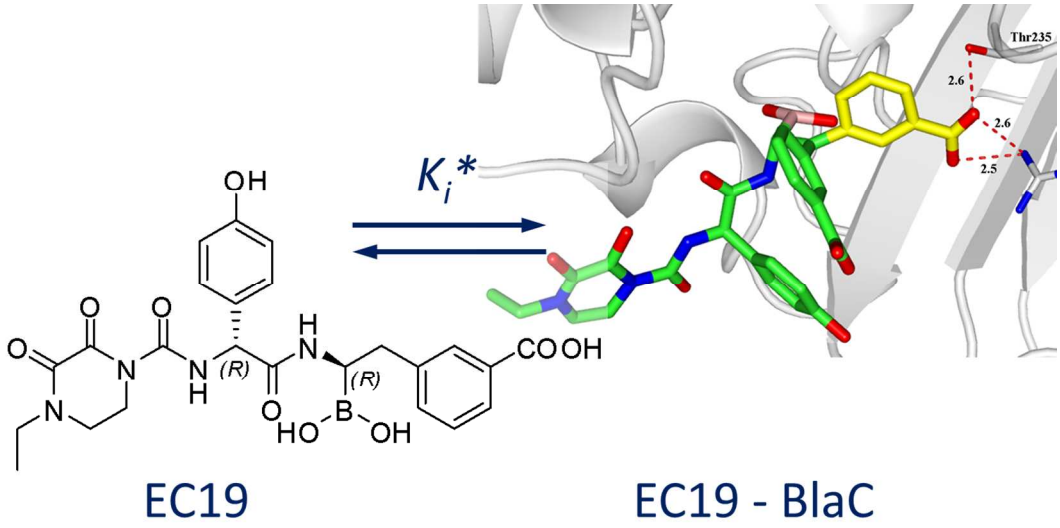

Currently, four-drug regimens are the cornerstone of treatment against infections with *Mycobacterium tuberculosis* (Mtb) achieving cure rates that approach 95% (1-3). Unfortunately, therapeutic challenges arise as a result of drug resistance. Due to the long treatment duration and the ability of *Mycobacteria* spp. to readily adapt to changes in their microenvironment, the emergence of resistance is inevitable. Against multi-drug resistant (MDR) and extensively drug resistant (XDR) strains of Mtb, chemotherapeutic choices are limited and new options are being sought (4). The concurrence of infection by Human Immunodeficiency Virus, HIV, and Mtb create a serious global challenge. Recent progress in antiretroviral therapy is hampered by increasing frequence of drug resistant strains of Mtb.

Presently, β-lactams, and their combination with β-lactam inhibitors, are being explored for the treatment of Mtb. The chromosomal β-lactamase, BlaC, is responsible for resistance to β-lactam antibiotics of multiple classes (5, 6). BlaC, which is capable of inactivating a broad range of penicillins and cephalosporins, belongs to Ambler class A, members of which usually being susceptible to inhibitors such as clavulanic acid (6). Indeed, the combination of meropenem and clavulanate was found to be effective in sterilizing Mtb cultures, including XDR strains (7). Furthermore, BlaC appears to be intolerant of substitutions that alter substrate profiles and confer resistance to clavulanic acid inactivation (8). Notwithstanding, a detailed understanding of structural determinants of effective inhibition may lead to development of more potent inhibitors. Based upon these considerations, we anticipate that novel β-lactamase inhibitors that possess favourable pharmacodynamic and pharmacokinetic properties will be effective against BlaC and will play an important role in treating drug-resistant Mtb infections in the near future (9).

Boronic acid transition state inhibitors (BATSIs) are a class of β-lactamase inhibitors, which have been studied and optimized for a variety of β-lactamase enzymes (10-15). By binding covalently to the active site nucleophile of the enzyme, the boronate adduct sterically and electronically resembles the tetrahedral high-energy intermediate of the β-lactam hydrolysis reaction. Such inhibitors have been shown to complex the active site and lead to inhibition in a reversible, competitive manner (Scheme 1). BATSIs can be synthesized so they possess a side-group which resembles R1 side-chains of known β-lactams necessary for specific interaction with the enzyme. Variation of this side-chain and the optional addition of an R2 group allow a rational inhibitor design (16).

In order to further elucidate the structural basis of effective inhibition, we used BATSIs to probe the active site of BlaC of Mtb. To this end, we tested a select panel of 25 BATSI compounds that carry different combinations of R1 and R2 side groups (Scheme 2), seven of which were newly synthesized. We determined key structural elements necessary for effective inhibition. We next expanded our analysis to variant enzymes with alterations in the carboxylate-binding regions. Our findings reveal that select BATSIs are effective biochemical inhibitors of BlaC, however they rely on productive interactions with the carboxylate binding region of the enzyme. These results allow for the potential design of a novel class of β-lactamase inhibitors to be used in the treatment of Mtb and expand our repertoire of possible compounds to be used in therapy.

RESULTS AND DISCUSSION

The design strategy employed here started with the two reference compounds shown in Figure 1. The acetyl group of **1** was systematically replaced with R1 substituents present on the β-lactam ring of active penicillin and cephalosporin-like antibacterials (compounds **3**-**21**). In addition a small number of ureido- and sulfonamido- derivatives were prepared (compounds **22**-**25**). These starting compounds were then further derivatized with one or two homologous *meta*-benzoic acid substituents (R2) to mimic the carboxylate group present on the larger heterocyclic fused ring of all β-lactam antibiotics. Finally, in the cefoperazone series, various phenolic, catecholic and aniline rings were introduced as substituents of the phenolic group of the R1 side chain.

The enzyme inhibition by BATSIs is posited to follow slow-reversible kinetics. Based on structural data, the model is represented according to the following equation (1):

$$E + I \leftrightarrow E{:}I \leftrightarrow E\text{-}I^{\neq} \leftrightarrow E\text{-}I^{\#\#} \quad (1)$$

where E stands for β-lactamase enzyme, I for inhibitor, E:I for the Michaelis complex, $E\text{-}I^{\neq}$ for enzyme-inhibitor complex resembling the acylation high-energy intermediate, and $E\text{-}I^{\#\#}$ the de-acylation high-energy intermediate, respectively. This model takes into account the crystallographic intermediates captured in SHV-1 (12), CTXM-9 and CTXM-14, respectively (13). Using the highly chromogenic nitrocefin as substrate, we screened these 25 compounds both under initial velocity conditions and after 5 minute pre-incubation with BlaC. Inhibitor concentrations that reduce the substrate reaction by 50% were determined and expressed as Ki values for immediate inhibitiory activity, and Ki* values following 5 minutes pre-incubation.

Both reference compounds **1** and **2** were devoid of inhibitory activity.

We identified eight with inhibitory activity, of which five inhibited BlaC at concentrations less than 5 μM. Almost all of these active inhibitors contained a *meta*-benzoic acid R2 substituent. The only exception was the cefotaxime analog, compound **11**; in our experiments this BATSI was a rapid onset inhibitor whose K_i value was 5.5 ± 0.3 μM, and only decreased to K_i* of 4.1 ± 0.3 μM after a five minute incubation with BlaC. All other seven active compounds revealed negligible activity when testing the inhibition immediately following BlaC addition, but revealed inhibition after a 5 minute pre-incubation with enzyme. The only penicillin analog with activity was the ampicillin analog**,** compound **3,** which possessed the benzoic acid R2 substituent. Of the cephalothin analogs, both compounds **9** and **10** showed activity. Both compounds also have benzoic acid R2 substituent, either directly attached to the boron-bearing carbon atom, or with a methylene spacer for additional flexibility. The ceftazidime analog, compound **13**, was a relatively weak inhibitor.

Of the eight cefoperazone analogs, only compounds **20** and **21** showed inhibitory activity after a five minute incubation with BlaC. This series explored different phenolic, catecholic and aniline substituents to evaluate whether changing the stereochemistry (compound **16**) and side chain length (compounds **15** and **17**) influenced inhibitory activity. Compounds **20** and **21**, like those in the cephalothin series, differed only in the spacing of the benzoic acid R2 substituent with respect to the boron atom. In this case, however, the added methylene group reduced the K_i* value five-fold, while in the cephalothin series, the opposite behavior was observed. Compound **21**, which we term EC19, exhibited the lowest K_i* value of all the BATSIs, with a measured K_i* value of 0.65 ± 0.05 μM.

Finally, a small number of ureido- and sulfonamido-containing boronic derivatives were prepared and evaluated. Only the ureido- compound **23** exhibited inhibitory activity. Neither sulfonamide compound (**24** and **25**) exhibited activity, including compound **25** which contains the benzoic acid R2 substituent. However, these compounds are known to adopt a different orientation of the R2 substituent when bound to the AmpC β-lactamase (17).

From these studies, we can make several general comments. Firstly, there is a clear and strong improvement in inhibition when there is a benzoic acid as the R2 substituent; we postulate that this group interacts with BlaC where the conserved carboxyl group present in all β-lactams binds. It is also clear that the presence of this substituent in the inhibitors induces time-dependent inhibitor kinetics that is not observed with the single inhibitory compound lacking this feature (compound **11**). Secondly, the nature of the R1 substituent influences, but is not the main driver of inhibitory activity. Different R1 groups were present in five different inhibitor series.

Our results are quite different from other reports of BATSI inhibition of other Class A and C β-lactamases. In the case of the *Acinetobacter*-derived ADC-7 cephalosporinase (15), the achiral cephalothin showed favorable inhibitory activity that was enhanced by the addition of a phenyl group in the R2 position. Similar observations have been reported for the TEM-1 β-lactamase (10). In the case of TEM-1, an aromatic R2 substituent allows for a favorable π-π stacking interaction with the Tyr105 phenolic ring (10). A tyrosine residue is found in the equivalent position in many Class A β-lactamases (18, 19). The KPC-2 carbapenemase has a tryptophan at the equivalent position that similarly stacks with aromatic substituents (20). The structures of a large number of BlaC-substrate and -inhibitor complexes reveals that aromatic amino acid side chains are not present in the active site at an equivalent position. This position is occupied by an isoleucine residue instead, which may explain the lack of activity of compound **7**. Rather, we believe that the effectiveness of the benzoic acid substituted BATSIs as BlaC inhibitors reflects their binding at the "carboxylate binding region" of the active site. This may differentiate BlaC from other Class A enzymes. In the crystal structure of BATSI covalently bound with the SHV-1 β-lactamase (12), the R1 substituent is found in an orientation in which it interacts with the carboxylate binding region.

To this end, we tested the inhibitory effectiveness of compound **21** (EC19) as inhibitor of variant forms of BlaC that possessed changes in the carboxylate binding pocket. In all previously characterized Class A β-lactamases, this region is repesented by a K234-T235-G236 sequence motif ("KTG motif") and a nearby arginine residue, R244 (21). In BlaC, the R244 is replaced with an alanine (A244). It was first shown for the TEM-1 β-lactamase, that this positive charge could be replaced by arginine residues located proximally to R244 (22). In the case of BlaC, the function of R244 is served by R220 which provides the necessary positive charge and electrostatically interacts with the negatively charged carboxylate of the β-lactam substrates (8). To investigate whether the R2 *meta*-benzoic acid substituent interacts with the carboxylate binding region of BlaC, we tested the inhibition of nitrocefin hydrolysis by the R220A, R220S and doubly substituted β-lactamase R220A, A244R (Table 2). These variants were constructed to investigate the impact of the positive charge (R220A, R220S) by relocalizing the positive charge from position 220 to 244. As a control, we also measured inhibition with the S130G variant enzyme which exhibits similar kinetic properties to the other variants but maintains the "native" carboxylate binding motif. Interestingly, we found that compound **21** is ineffective at inhibiting the R220A and R220S variants of BlaC, yet retains potent inhibition against both the doubly substituted β-lactamase where the positive charge has been repositioned from residue 220 to residue 244 and the S130G BlaC retaining the native carboxylate binding site. These data argue

that the *meta*-benzoic acid R2 substituent binds as a mimic of the substrate carboxylate. Further, these observations may point towards a potential mechanism to develop resistance against BATSI compounds.

Essentially, almost all of the active BATSIs exhibit time-dependent inactivation, a behavior that has been previously observed for other β-lactamases when inhibited with BATSIs that carry a stereogenic center (23, 24). In order to investigate this more thoroughly, we performed experiments in which the hydrolysis of nitrocefin by BlaC was determined as a function of inhibitor concentration, focusing upon EC19 (compound **21**). As seen in Figure S1A, the initial rates are approximately similar at various EC19 concentrations, but after 150-200 seconds the rates begin to decrease and, at higher concentrations, the reaction rates approach zero. These data were fit to a model where the inhibitors bind to the free BlaC and form an initial Michaelis complex, which then isomerizes in a slow step to generate a second complex. Using equation 4, we could calculate from these data values for k_{on} of 0.001 $\mu M^{-1}s^{-1}$ and k_{off} of 0.0013 sec^{-1} (our chemical interpretation of this kinetic model will be discussed below). To test whether this time dependency also applied to dissociation of the inhibitor from the complex, and to ensure the covalent complex was reversibly formed, we formed the complex (10x the K_i*) and tested for inhibitor release and regain of activity by diluting the complex 100-fold before adding nitrocefin to initiate the reaction. Using EC19, the reaction rate increased slowly, consistent with a reversible but very slow dissociation rate (Figure S2A). In contrast, when this experiment was performed with LP08 (compound **11**), the rate of hydrolysis of nitrocefin was essentially equal to the control reaction, where inhibitor was not added (Figure S2A). These kinetic results support our proposal that the time-dependence of BATSIs containing the *meta*-benzoic acid R2 substituent is due to this binding and subsequent isomerization both in the association and dissociation reactions.

Finally, the influence of the R1 substituent on inhibitory potency is not mirrored in the efficiency of the corresponding β-lactam as substrate for BlaC. Penicillins are in general better substrates for BlaC than cephalosporins (6, 25). For example, ampicillin exhibits a K_m value of 8 μM (6, 25), yet compound **3** exhibits one of the highest K_i* values of all active compounds tested. Cephalothin exhibits a K_m value of 150 μM; however compound **10** exhibits a K_i* value of 2.7 ± 0.2 μM. Finally, cefotaxime exhibits a K_m value of 5.5 mM, yet compound **11** exhibits a K_i* value of 5.5 ± 0.3 μM. Similar observations have been reported for the Class A extended spectrum β-lactamase CTX-M: the most potent BATSI inhibitor contained the R1 substituent of ceftazidime, one of the enzymes least favorable substrates (13). To see if this observation holds true for BlaC and cefoperazone, we evaluated cefoperazone as a substrate for BlaC: We did not detect any hydrolysis when testing concentrations up to 100 μM. Further, we tested to see whether this compound was a "slow substrate" for BlaC and thus an inhibitor of nitrocefin hydrolysis. Cefoperazone at a concentration of 10 μM did not inhibit nitrocefin hydrolysis. We hypothesize that the rigid structure of cefoperazone, with the dihydrothiazine ring fused to the β-lactam ring, may prevent the optimal interaction of both the carboxylate and the R1 substituent. In the case of the BATSI inhibitors described here, the *meta*-benzoic acid R2 substituent and R1 diketopiperazine are connected by bonds that allow for free rotation of the two groups, thus allowing for optimal alignment and interaction within the BlaC active site. In this setting, the more complex R1 substituents of the cephalosporins may allow for more specific interactions with BlaC that complement the interaction of the β-lactam carboxylate with the carboxylate

binding site. In a broader view, BATSI inhibitors are not mimicking the natural substrate of the enzyme, but rather the high energy intermediate product of the enzymatic reaction.

Crystal structure

Co-crystallisation of wild type BlaC with EC19 was prevented by the dissolution of the crystal in DMSO containing inhibitor solution. However, the compound was successfully trapped in the N172A variant protein which additionally resulted in bigger crystals and the structure was resolved at 1.4 Å. There was clear electron density between the Ser70 hydroxyl side chain and the boron atom in the boronate covalent complex of EC19 and BlaC. All three rings of the inhibitor were able to be unambiguously mapped and Figure 2A shows the model of the bound complex surrounded by the experimental electron density, contoured at 2σ.

One of the boronate oxygen atoms interacts with the amide nitrogens of Ser70 and Thr237 (Figure 2B). These two residues constitute the "oxyanion hole" that stabilizes the formation of the anionic, tetrahedral intermediate during β-lactam hydrolysis (Scheme 1). The other boronate oxygen occupies the position where the conserved hydrolytic water molecule normally is located. The boronate oxygen atom makes a hydrogen bonding interaction with Glu166, the base normally responsible for activating the water molecule in the deacylation reaction. The diketopiperazine substituent (R1) makes several interactions with active site residues. The two ketones are positioned by hydrogen bonding to the amide backbone nitrogens of Ser104 and Arg103 while the nearby exocyclic carbonyl interacts with the side chain of Arg171. The central phenol ring points out into solvent and makes a hydrogen bonding interaction with a water molecule. The *meta*-benzoic acid R2 substituent similarly points out toward solvent and makes no interactions with the enzyme. However, clearly defined electron density is observed in the complex where the carboxylate of other β-lactam complexes normally binds. We have modelled this as a phosphate anion in Figure 2B, since the crystallization solution contains 2 M sodium phosphate and this phosphate anion has been observed at this position in the apo-BlaC structure (PDB entry 2GDN).

Based on this additional electron density, we advance that in solution, the binding of EC19, and other similarly substituted inhibitors, is driven by the interaction of the carboxyl group with R220 and T235, residues that make up the carboxylate binding site. We could obtain a reasonable model of that interaction by simply rotating the methylene group of the *meta*-benzoic acid substituent to optimize the interaction between the carboxyl group and R220 and T235 (Figure 3). This generates two quite reasonable hydrogen bonds at distances of 2.3 and 2.6 Å, respectively. We propose, based on the nature and strength of the inhibition by the inhibitor series studied here, that the initial interaction between EC19 and the enzyme is driven by the binding of the *meta*-benzoic acid group into the carboxyl binding site. This interaction is similar to the formation of a pre-catalytic Michaelis complex for substrates and positions the boronate atom in proximity to S70 which, after deprotonation by K73, adds as a nucleophile to the boron atom to generate the covalent enzyme-inhibitor complex. The two boronate oxygen atoms interact with the oxyanion hole residues and the E166 catalytic base in the deacylation reaction. This is followed by the interaction of the diketopiperazine substituent with the amide backbone nitrogens of R103 and S104 and of the carbonyl group with R171. In solution, it is likely that the *meta*-benzoic acid substituent remains bound at the carboxylate binding site, and that the alternate inhibitor conformation that we observe in the crystal is likely due to the very high

concentration of phosphate in the crystallization buffer solution and the inability of the EC19 benzoic acid substituent to displace it.

Conclusion:

We show here that BATSIs can be used as molecular probes to investigate the structural basis of inhibition of BlaC, an important drug target against otherwise drug resistant strains of tuberculosis. Our major observation is that in addition to a R1 group, the *meta*-benzoic acid substituent in R2 position is necessary for effective inhibition of BlaC, as it provides productive interactions with the carboxylate binding region of the enzyme. Compound **21** (EC19) was found to have a K_i* of 0.65μM, which is lower than corresponding values for currently available inhibitors (we have determined the IC_{50} of clavulanate, sulbactam, and tazobactam as 1.7 ± 0.2, 1.6 ± 0.2, and 2.5 ± 0.2 μM, respectively (8)). This is the first description of a BATSI inhibitor against BlaC. EC19 may serve as an important lead compound for the rational design of more potent inhibitors. With the insights obtained by this structure-function study, we are confident that further optimisation can be reached.

METHODS:

BlaC purification

The *blaC* genes carrying a truncated sequence of BlaC cloned in a pET28 based plasmid was expressed in *E. coli* BL21(DE3) and purified; the correct size was confirmed by mass spectrometry as previously described (6, 8). Variant enzymes were generated using site-directed mutagenesis as reported (8, 26). Protein concentrations were determined measuring absorption at 280nm at various dilutions using an Eppendorf BioPhotometer plus (Eppendorf AG Hamburg, Germany).

BATSI synthesis

BATSIs were chemically synthesized by acylation of aminomethaneboronate with suitable commercially-available R1-carboxylic acids. Chiral BATSIs were obtained in enantiomerically pure form by stereoselective homologation of (+)-pinanediol 3-carboxyphenyl-methaneboronate followed by substitution, acylation and final deprotection at the boronic and carboxylic functionalities. The general scheme for the synthesis of these compounds is summarized in Scheme 2 and experimental details for the synthesis of BATSIs are reported in Supplementary Material (Compounds **2**, **5**, **8**, **18**, **20**, **22** and **23**) or elsewhere (see Table 1).

Kinetic measurements

Steady state kinetics were performed on an Agilent 8453 diode array spectrophotometer (Palo Alto, CA) in Na-Phosphate buffer at room temperature (50 mM, pH 7.2) and a 1cm path length cuvette as previously detailed. Nitrocefin (NCF) was used as substrate with the extinction coefficient $\Delta\varepsilon$ =17,400 $M^{-1}cm^{-1}$ at 482 nm. Inhibitor kinetics were performed with NCF as the reporter substrate at 100 μM concentration. BATSIs follow reversible inhibition kinetics. Increasing concentrations were used to determine the specific concentration K_i that reduces initial NCF hydrolysis reaction by 50%. For each concentration reactions were performed in triplicates and the average velocity was used. Results were corrected for NCF affinity using equation (2):

$$K_i(\text{corrected}) = K_i(\text{obs})/(1 + [\text{NCF}]/K_{\text{mNCF}}) \quad (2)$$

Kinetic parameters for BlaC and the reporter substrate NCF were previously determined as K_m 56 μM and k_{cat} 72 sec^{-1} (8). This corresponds to a correction factor of 0.36.

In a first screen, 50 μM of inhibitor were used to determine compounds with the ability to reduce the initial velocity of nitrocefin hydrolysis by BlaC by 50%, which would correspond to a "K_i corrected" of 20 μM or less. For all compounds, initial velocities were obtained within 5 seconds and after 5 minutes pre-incubation. For compounds that possess a stereogenic center on the boron-bearing carbon atom we gererally observed slow, reversible inactivation resulting in a substantial increase in inhibition after 5 minute pre-incubations. For compounds which reduced initial velocities by at least half, formal determination of K_i (immediate) and K_i* (5 minutes pre-incubation), respectively, was performed. The results are summarized in Table 1.

In select cases (i.e., compound **21** (EC19)), testing for reversibility of inhibition was performed as follows: 0.05 μg BlaC was incubated in total of 10 μl buffer with the inhibitor at concentration equal to 10 x K_i* for 20 min. Then, the whole reaction mix was added to 990 μl buffer solution containing 100μM NCF, equal to 1:100 dilution of inhibitor (0.1 x K_i*). The

formation of the NCF product of hydrolysis over 800s was monitored and compared to a similar experiment without inhibitor.

For EC19, association and dissociation rate constants (k_{on} and k_{off}, respectively) were determined as follows: Product formation was monitored over time in the presence of EC19 in increasing concentrations using 0.05 μg BlaC and 100 μM NCF. The data were fitted to equation 3 using Origin 8.0 (OriginLab, Northampton, MA) to obtain the apparent rate constant k_{obs}, which reflects the rate for conversion from initial velocity (v_i) phase to steady state velocity (v_s), with $A(t)$ indicating absorbance at reaction time t, and A_0 initial absorbance, respectively:

$$A(t) = A_0 + v_s t + (v_i - v_s)/k_{obs} * [1 - \exp(-k_{obs} t)] \quad (3)$$

For simple (one step) reversible binding to BlaC, k_{obs} is a linear function of inhibitor concentration (eq. 4), with:

$$k_{obs} = k_{on}[I] + k_{off} \quad (4).$$

Thus, k_{off} is the y(0) intercept, and k_{on} is derived from the slope $k_{obs}/[I]$, corrected for affinity (eq. 5)(27):

$$k_{on} = k_{obs}/[I] * (1 + [S]/K_m) \quad (5)$$

An inhibition screen with two compounds (20μM) was performed for the BlaC variant enzymes R220A, R220S, R220A-A244R and S130G in order to determine the impact of the carboxylate binding site (8). The results are summarized in Table 2.

Crystallography

The method of hanging drop vapour diffusion was used for crystallization of N172A mutant BlaC. The composition of the well consists of 0.1 M HEPES, pH 7.5 and 2 M $NH_4H_2PO_4$, which makes the final pH of the well solution, 4.1. Protein at a concentration of 14 mg/ml was mixed 1:1 with the well solution and incubated at 10 °C. The N172A BlaC was initially seeded with the native enzyme crystals (BlaC) and then after iterative crystal seeding, the pure mutant crystals were obtained. Iterative micro-seeding resulted in efficient crystal growth as well as improved morphology and finally produced diffraction quality crystals of the mutant enzyme. N172A crystals were solved in same space group ($P2_12_12_1$) as the wild type and were bigger in size.

Data Collection and Refinement: EC19 is insoluble in water, but soluble in DMSO. A DMSO solution of 500 mM EC19 was used as a stock solution and serially diluted with equal volume of water for three rounds of soaking. This diluted DMSO solution (containing about 65 mM EC19) was used for soaking experiment with N172A variant BlaC. After placement in the soaking solution, the crystals were frozen in liquid nitrogen in time intervals of 15 minutes, 30 minutes, 1, 2, 4, 6, 12, 24 and 48 hours respectively. Mineral oil was added to the solution as a cryo-protectant. Diffraction data were collected from each of the single frozen crystals using a RAXIS-IV++ detector mount on a Rigaku RH-200 rotating anode (copper anode) X-ray generator. While no or insufficient electron density of the ligand was observed for crystals after early freezing, adequate intensity was observed for crystals frozen after 24 hours of soaking. Data were collected at Brookhaven National Laboratory on crystals frozen after 24 hours soaking with EC19. Beam lines X29 were used for data collection. The data were processed using

HKL2000 (28). Previous structure of Mtb β-lactamase with bound NXL104 (PDB entry 4HFX) (29) was used to phase the data, using the CCP4 software suite (30). Multiple rounds of structural refinement and model building were performed in Refmac5 (31, 32), Phenix (33) and Coot (34). Structure figures were generated using PyMOL (The PyMOL Molecular Graphics System, Version 1.3, Schrödinger, LLC.) and ChemDraw Ultra 12.0 *(35)*. Atomic coordinates and experimental structure factors have been deposited in the Protein Data Bank (PDB entry 4X6T). Table 3 lists the data collection statistics for the structures as well as the final refinement statistics

ACKNOWLEDGEMENT

Research reported in this publication was supported by the National Institute of Allergy and Infectious Diseases of the National Institutes of Health under Award Numbers R01AI100560 and R01AI063517 (to RAB) and NIH AI060899 (to J.S.B.). The content is solely the responsibility of the authors and does not necessarily represent the official views of the National Institutes of Health. This study was supported in part by funds and/or facilities provided by the Cleveland Department of Veterans Affairs, the Veterans Affairs Merit Review Program Award 1I01BX001974 and the Geriatric Research Education and Clinical Center VISN 10 (to RAB).
Parts of this study were presented in form of an Abstract (European Congress of Clinical Microbiology and Infectious Diseases, Milan 2011, American Thoracic Society, San Diego 2014).

Supplementary Information:

Supporting Information includes Figures S1A, B & S2A, B and descriptions of the synthesis of compounds. This material is free of charge via the Internet at http://pubs.acs.org.

Accession Code. The Protein Data Bank entry for the BlaC-EC19 adduct is **4X6T**.

References

1. Hong-Kong-Chest-Service/British-Medical-Research-Council. (1991) Controlled trial of 2, 4, and 6 months of pyrazinamide in 6-month, three-times-weekly regimens for smear-positive pulmonary tuberculosis, including an assessment of a combined preparation of isoniazid, rifampin, and pyrazinamide. Results at 30 months. Hong Kong Chest Service/British Medical Research Council, *Am Rev Respir Dis 143*, 700-706.
2. Singapore-Tuberculosis-Service/British-Medical-Research-Council (1991) Assessment of a daily combined preparation of isoniazid, rifampin, and pyrazinamide in a controlled trial of three 6-month regimens for smear-positive pulmonary tuberculosis. Singapore Tuberculosis Service/British Medical Research Council, *Am Rev Respir Dis 143*, 707-712.
3. Combs, D. L., O'Brien, R. J., and Geiter, L. J. (1990) USPHS Tuberculosis Short-Course Chemotherapy Trial 21: effectiveness, toxicity, and acceptability. The report of final results, *Ann Intern Med 112*, 397-406.
4. WHO (2010) *Multidrug and extensively drug-resistant TB (M/XDR-TB): 2010 global report on surveillance and response.*
5. Chambers, H. F., Moreau, D., Yajko, D., Miick, C., Wagner, C., Hackbarth, C., Kocagoz, S., Rosenberg, E., Hadley, W. K., and Nikaido, H. (1995) Can penicillins and other beta-lactam antibiotics be used to treat tuberculosis?, *Antimicrob Agents Chemother 39*, 2620-2624.
6. Wang, F., Cassidy, C., and Sacchettini, J. C. (2006) Crystal structure and activity studies of the Mycobacterium tuberculosis beta-lactamase reveal its critical role in resistance to beta-lactam antibiotics, *Antimicrob Agents Chemother 50*, 2762-2771.
7. Hugonnet, J. E., Tremblay, L. W., Boshoff, H. I., Barry, C. E., 3rd, and Blanchard, J. S. (2009) Meropenem-clavulanate is effective against extensively drug-resistant Mycobacterium tuberculosis, *Science 323*, 1215-1218.
8. Kurz, S. G., Wolff, K. A., Hazra, S., Bethel, C. R., Hujer, A. M., Smith, K. M., Xu, Y., Tremblay, L. W., Blanchard, J. S., Nguyen, L., and Bonomo, R. A. (2013) Can Inhibitor-Resistant Substitutions in the Mycobacterium tuberculosis beta-Lactamase BlaC Lead to Clavulanate Resistance?: a Biochemical Rationale for the Use of beta-Lactam-beta-Lactamase Inhibitor Combinations, *Antimicrob Agents Chemother 57*, 6085-6096.
9. Kurz, S. G., and Bonomo, R. A. Reappraising the use of beta-lactams to treat tuberculosis, *Expert Rev Anti Infect Ther 10*, 999-1006.
10. Ness, S., Martin, R., Kindler, A. M., Paetzel, M., Gold, M., Jensen, S. E., Jones, J. B., and Strynadka, N. C. (2000) Structure-based design guides the improved efficacy of deacylation transition state analogue inhibitors of TEM-1 beta-Lactamase(,), *Biochemistry 39*, 5312-5321.
11. Thomson, J. M., Prati, F., Bethel, C. R., and Bonomo, R. A. (2007) Use of novel boronic acid transition state inhibitors to probe substrate affinity in SHV-type extended-spectrum beta-lactamases, *Antimicrob Agents Chemother 51*, 1577-1579.
12. Ke, W., Sampson, J. M., Ori, C., Prati, F., Drawz, S. M., Bethel, C. R., Bonomo, R. A., and van den Akker, F. (2011) Novel insights into the mode of inhibition of class A SHV-1

beta-lactamases revealed by boronic acid transition state inhibitors, *Antimicrob Agents Chemother 55*, 174-183.

13. Chen, Y., Shoichet, B., and Bonnet, R. (2005) Structure, function, and inhibition along the reaction coordinate of CTX-M beta-lactamases, *J Am Chem Soc 127*, 5423-5434.
14. Morandi, F., Caselli, E., Morandi, S., Focia, P. J., Blazquez, J., Shoichet, B. K., and Prati, F. (2003) Nanomolar inhibitors of AmpC beta-lactamase, *J Am Chem Soc 125*, 685-695.
15. Drawz, S. M., Babic, M., Bethel, C. R., Taracila, M., Distler, A. M., Ori, C., Caselli, E., Prati, F., and Bonomo, R. A. (2010) Inhibition of the class C beta-lactamase from Acinetobacter spp.: insights into effective inhibitor design, *Biochemistry 49*, 329-340.
16. Morandi, S., Morandi, F., Caselli, E., Shoichet, B. K., and Prati, F. (2008) Structure-based optimization of cephalothin-analogue boronic acids as beta-lactamase inhibitors, *Bioorg Med Chem 16*, 1195-1205.
17. Eidam, O., Romagnoli, C., Caselli, E., Babaoglu, K., Pohlhaus, D. T., Karpiak, J., Bonnet, R., Shoichet, B. K., and Prati, F. (2010) Design, synthesis, crystal structures, and antimicrobial activity of sulfonamide boronic acids as beta-lactamase inhibitors, *J Med Chem 53*, 7852-7863.
18. Doucet, N., De Wals, P. Y., and Pelletier, J. N. (2004) Site-saturation mutagenesis of Tyr-105 reveals its importance in substrate stabilization and discrimination in TEM-1 beta-lactamase, *J Biol Chem 279*, 46295-46303.
19. Bethel, C. R., Hujer, A. M., Hujer, K. M., Thomson, J. M., Ruszczycky, M. W., Anderson, V. E., Pusztai-Carey, M., Taracila, M., Helfand, M. S., and Bonomo, R. A. (2006) Role of Asp104 in the SHV beta-lactamase, *Antimicrob Agents Chemother 50*, 4124-4131.
20. Ke, W., Bethel, C. R., Thomson, J. M., Bonomo, R. A., and van den Akker, F. (2007) Crystal structure of KPC-2: insights into carbapenemase activity in class A beta-lactamases, *Biochemistry 46*, 5732-5740.
21. Drawz, S. M., and Bonomo, R. A. (2010) Three decades of beta-lactamase inhibitors, *Clin Microbiol Rev 23*, 160-201.
22. Marciano, D. C., Brown, N. G., and Palzkill, T. (2009) Analysis of the plasticity of location of the Arg244 positive charge within the active site of the TEM-1 beta-lactamase, *Protein Sci 18*, 2080-2089.
23. Wang, X., Minasov, G., Blazquez, J., Caselli, E., Prati, F., and Shoichet, B. K. (2003) Recognition and resistance in TEM beta-lactamase, *Biochemistry 42*, 8434-8444.
24. Thomson, J. M., Distler, A. M., Prati, F., and Bonomo, R. A. (2006) Probing active site chemistry in SHV beta-lactamase variants at Ambler position 244. Understanding unique properties of inhibitor resistance, *J Biol Chem 281*, 26734-26744.
25. Hugonnet, J. E., and Blanchard, J. S. (2007) Irreversible inhibition of the Mycobacterium tuberculosis beta-lactamase by clavulanate, *Biochemistry 46*, 11998-12004.
26. Hujer, A. M., Hujer, K. M., Helfand, M. S., Anderson, V. E., and Bonomo, R. A. (2002) Amino acid substitutions at Ambler position Gly238 in the SHV-1 beta-lactamase: exploring sequence requirements for resistance to penicillins and cephalosporins, *Antimicrob Agents Chemother 46*, 3971-3977.
27. Copeland, R. A. (2005) *Evaluation of Enzyme Inhibitors in Drug Discovbery*, John Wiley & Sons, Inc.
28. Otwinowski, Z., and Minor, W. (1997) Processing of X-ray Diffraction Data Collected in Oscillation Mode, *Methods in Enzymology 276*, 307-326.

29. Xu, H., Hazra, S., and Blanchard, J. S. (2012) NXL104 irreversibly inhibits the beta-lactamase from Mycobacterium tuberculosis, *Biochemistry 51*, 4551-4557.
30. Potterton, E., Briggs, P., Turkenburg, M., and Dodson, E. (2003) A graphical user interface to the CCP4 program suite, *Acta Crystallogr D Biol Crystallogr 59*, 1131-1137.
31. Murshudov, G. N., Vagin, A. A., and Dodson, E. J. (1997) Refinement of macromolecular structures by the maximum-likelihood method, *Acta Crystallogr D Biol Crystallogr 53*, 240-255.
32. Pannu, N. S., Murshudov, G. N., Dodson, E. J., and Read, R. J. (1998) Incorporation of prior phase information strengthens maximum-likelihood structure refinement, *Acta Crystallogr D Biol Crystallogr 54*, 1285-1294.
33. Adams, P. D., Afonine, P. V., Bunkoczi, G., Chen, V. B., Davis, I. W., Echols, N., Headd, J. J., Hung, L. W., Kapral, G. J., Grosse-Kunstleve, R. W., McCoy, A. J., Moriarty, N. W., Oeffner, R., Read, R. J., Richardson, D. C., Richardson, J. S., Terwilliger, T. C., and Zwart, P. H. (2010) PHENIX: a comprehensive Python-based system for macromolecular structure solution, *Acta Crystallogr D Biol Crystallogr 66*, 213-221.
34. Emsley, P., and Cowtan, K. (2004) Coot: model-building tools for molecular graphics, *Acta Crystallogr D Biol Crystallogr 60*, 2126-2132.
35. Mills, N. (2006) ChemDraw Ultra 10.0, *J. Am. Chem. Soc. 128*, 13649-13650.
36. Winkler, M. L., Rodkey, E. A., Taracila, M. A., Drawz, S. M., Bethel, C. R., Papp-Wallace, K. M., Smith, K. M., Xu, Y., Dwulit-Smith, J. R., Romagnoli, C., Caselli, E., Prati, F., van den Akker, F., and Bonomo, R. A. (2013) Design and exploration of novel boronic acid inhibitors reveals important interactions with a clavulanic acid-resistant sulfhydryl-variable (SHV) beta-lactamase, *J Med Chem 56*, 1084-1097.
37. Kotsakis, S. D., Caselli, E., Tzouvelekis, L. S., Petinaki, E., Prati, F., and Miriagou, V. (2013) Interactions of oximino-substituted boronic acids and beta-lactams with the CMY-2-derived extended-spectrum cephalosporinases CMY-30 and CMY-42, *Antimicrob Agents Chemother 57*, 968-976.

Table 1: Compounds and their corresponding inhibitor constants: K_i is the inhibitor concentration that results in 50% velocity reduction of NCF hydrolysis, corrected for substrate affinity. K_i* is the corresponding concentration in μM, obtained after pre-incubation of the enzyme with inhibitor over 5 minutes (mean of three experiments with standard error). * indicates compounds that bear two, R1 and R2, side groups (compounds with a stereogenic center).

Number	Ref	Inhibitor	K_i(μM)	K_i*(μM)
	Reference compounds			
1	(11)	LP03	>20	>20
2	-	EC6803	>20	>20
	Penicillin series			
3	(36)	EC25 (Ampicillin)*	>20	13.2 ±1.7
4	(36)	GB21 (Nafcillin)	>20	>20
5	-	FP2107 (Oxacillin)	>20	>20
	Cephalothin series			
6	(16)	LP04	>20	>20
7	(16)	FP2807*	>20	>20
8	-	CR126*	>20	>20
9	(*24*)	SM23*	>20	1.46 ±0.2
10	(*17*)	EC04	>20	2.76 ±0.2
	Cefotaxim compound			
11	(11)	LP08	5.54 ±0.3	4.13 ±0.3
	Ceftazidime series			
12	(15)	LP06	>20	>20
13	(37)	MC35*	>20	17.7 ±2.0
	Cefoperazone series			
14	(12)	GB0301	>20	>20
15	(12)	EC7406	>20	>20
16	(12)	EC9901	>20	>20
17	(12)	EC9701	>20	>20
18	-	EC9001	>20	>20
19	(15)	CR102	>20	>20
20	-	COBOR10*	>20	3.34 ±0.4
21	(36)	EC19*	>20	0.65 ±0.05
	Ureido and sulfonamido compounds			
22	-	CR48	>20	>20
23	-	FP110216*	>20	7.17 ±0.4
24	(*17*)	CR23	>20	>20
25	(*17*)	CR100	>20	>20

Table 2: BlaC site-directed variant enzymes: Fractional velocities (v/v_0) of NCF hydrolysis following 5 minutes pre-incubation with inhibitor EC19 at 20 μM concentration, in relation to uninhibited reaction, performed in triplicates. Note that the catalytic efficiency of the variant enzymes is significantly impaired compared to the wild type, with kcat/Km ratios (in $\mu M^{-1}\ s^{-1}$)

for NCF of 0.01 (R220A, R220S0, 0.02 (S140G), and 0.1 (R220A, A244R), and 1.34 (wild type), respectively (8). S130G variant enzyme was completely inhibited by EC19.

	EC19 (**21**)
R220A	0.96 ± 0.3
R220S	0.96 ± 0.2
R220A, A244R	0.37 ± 0.2
S130G	<0.1

Table 3: Summary of data collection and refinement statistic for the N186Ala -BlaC-EC19 Complex

Data Collection statistics:	
X-Ray Source	NSLS Beamline X-29
Date of Collection	2013-09-20
Wavelength (Å)	1.0 (Single Wavelength)
Temperature (K)	100
Resolution Range	38.5-1.40
Reflection	50722
Completeness	91.67 (100)
Redundancy	6.5
I/Sigma (σ)	3.05
Space Group	$P2_12_12_1$
Unit Cell (Å)	
A	43.26
B	71.42
C	84.68
α=β=ϒ	90.00°
Molecules per a.u.	1
Refinement	
Refinement Program	PHENIX
R_{work} (%)	16.60
R_{free} (%)	20.20
$R_{free\ Test\ Set}$	1993 Reflections (4.13%)
Estimated Twining Fraction	No Twining to report
Atoms	
Total number of Atoms	2341
Average B Factor	20.0
Protein (Chain A)	2005
Phosphate (Chain P)	35
EC19 (Chain E)	38
Water (Chain W)	263
r.m.s. Deviation	
Bond Length (Å)	0.006
Bond Angle (°)	1.283
PDB Accession Code	**4X6T**

Scheme 1: Mechanism of Boronic acid Transition State Inhibitors. The top row shows the formation of the tetrahedral high-energy intermediate of the cefotaxime-hydrolysis reaction. The bottom row shows the boronate complex formation of a cefotaxime-BATSI which resembles the tetrahedral high-energy intermediate.

Scheme 2: General scheme for the synthesis of BATSI compounds. See references in Table 1 and supplementary information for details.

Figure 1: The structures and inhibition constants of the compounds tested as inhibitors of BlaC.

Figure 2: Crystal structure of BlaC with EC19 bound at the active site. Inhibitor atoms are colored by atom type. (A) Structure of EC19 (left) and EC19 modelled into the F_o-F_c omit map contoured at 2.0 σ. (B) Electrostatic interactions between covalently bound EC19 and BlaC.

Figure 3: Proposed mode of binding of EC19 with BlaC in solution. Only a modest rotation of the methylene group connecting the boron atom and the meta-benzoic acid substituent results in two hydrogen bonds formed to the side chain of Arg220 and Thr235.

Scheme 1:

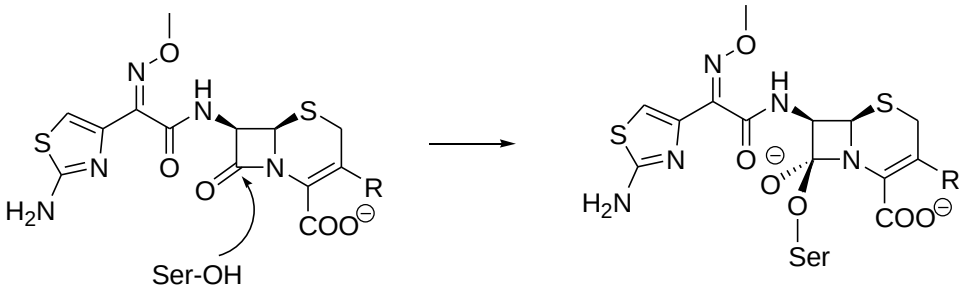

Cefotaxime + E

High-energy intermediate

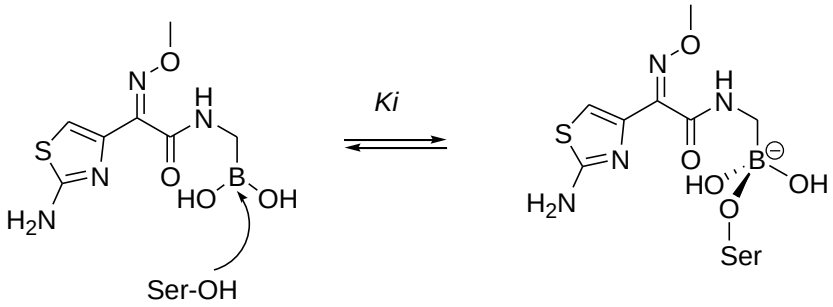

Cefotaxime-BATSI + E

Boronate complex

Scheme 2

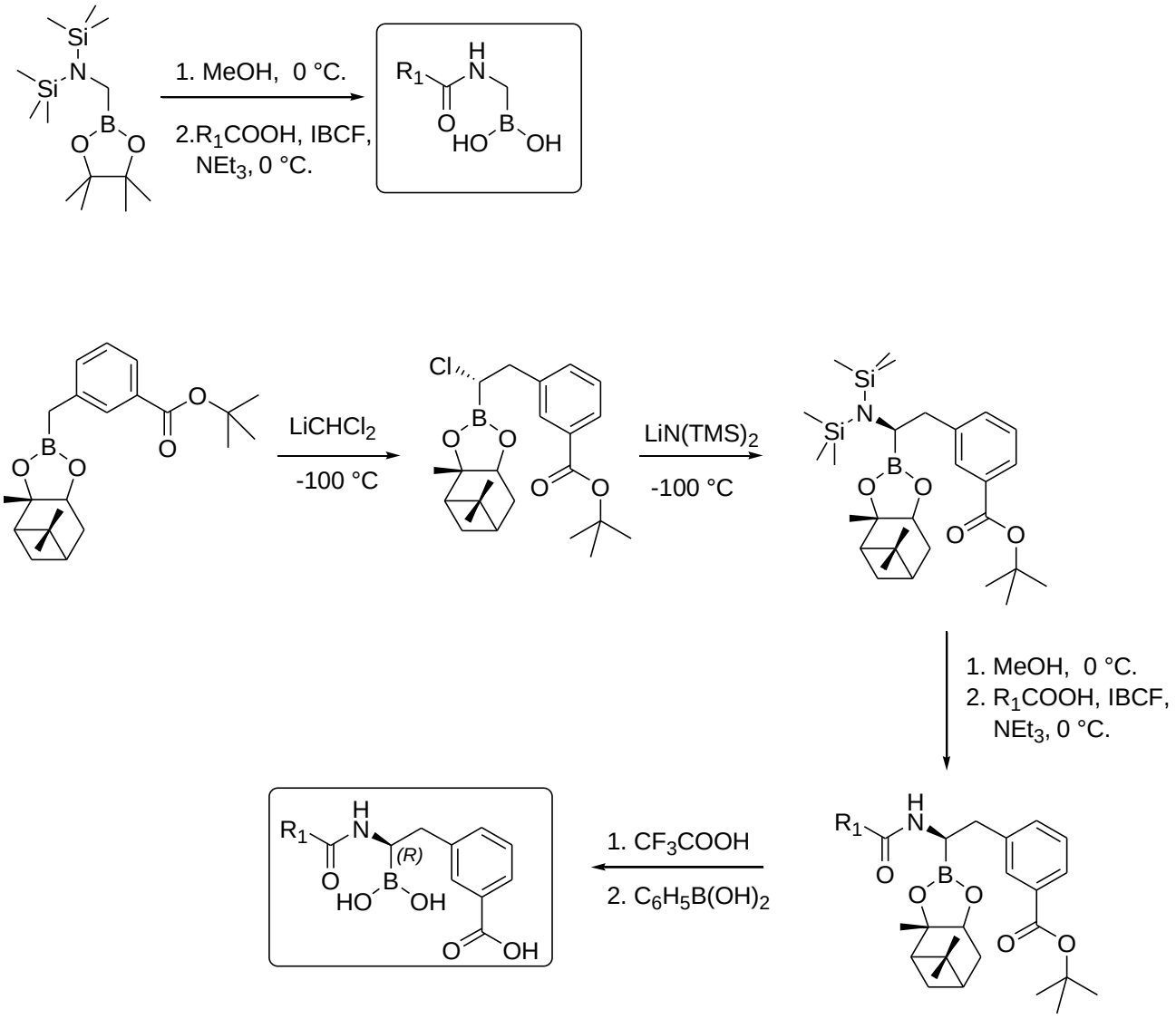
1. MeOH, 0 °C.
2.R1COOH, IBCF, NEt3, 0 °C.
LiCHCl2
-100 °C
LiN(TMS)2
-100 °C
1. MeOH, 0 °C.
2. R1COOH, IBCF, NEt3, 0 °C.
1. CF3COOH
2. C6H5B(OH)2

Figure 1

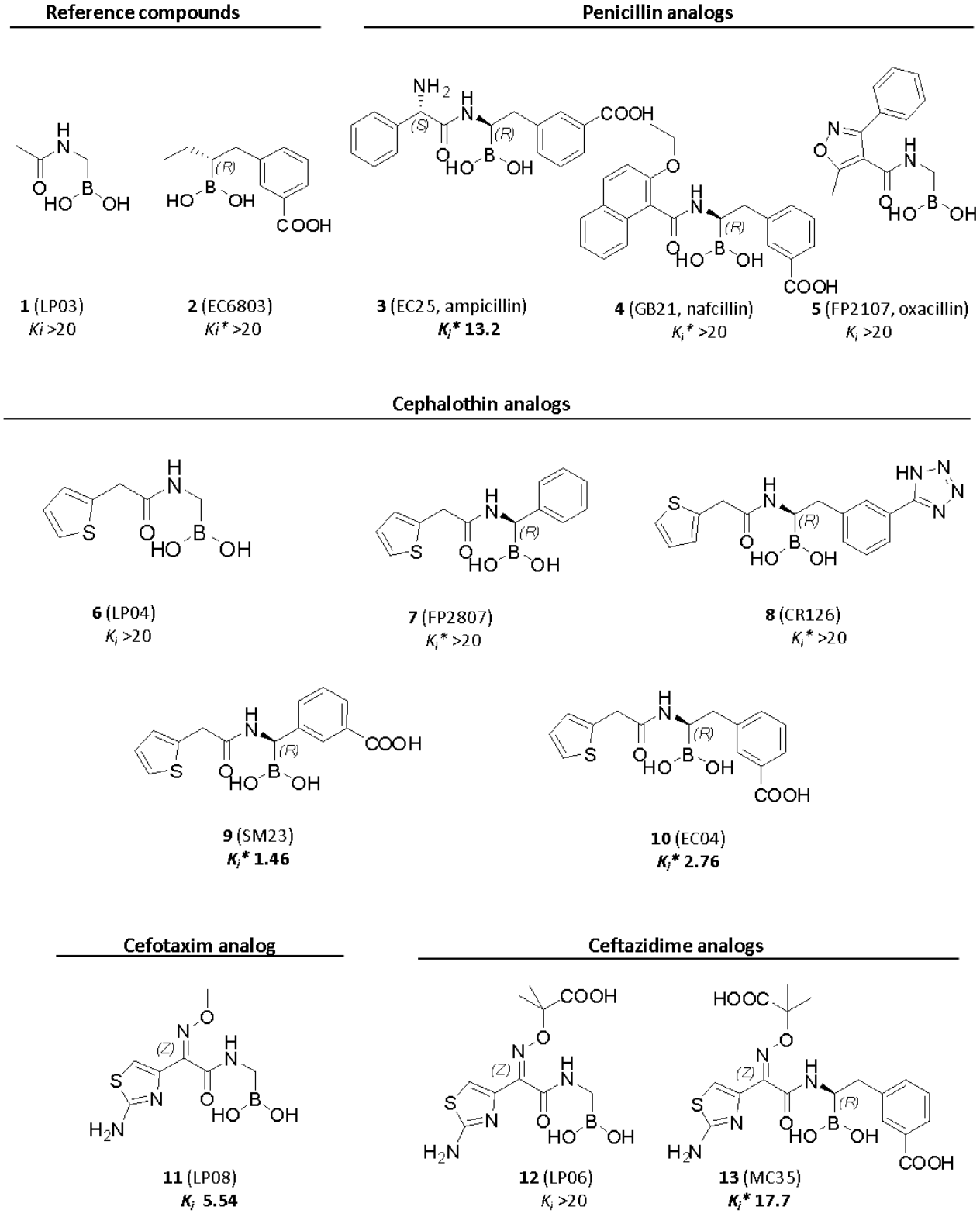
Reference compounds
Penicillin analogs
1 (LP03)
Ki >20
2 (EC6803)
Ki* >20
3 (EC25, ampicillin)
Ki* 13.2
4 (GB21, nafcillin)
Ki* >20
5 (FP2107, oxacillin)
Ki >20
Cephalothin analogs
6 (LP04)
Ki >20
7 (FP2807)
Ki* >20
8 (CR126)
Ki* >20
9 (SM23)
Ki* 1.46
10 (EC04)
Ki* 2.76
Cefotaxim analog
Ceftazidime analogs
11 (LP08)
Ki 5.54
12 (LP06)
Ki >20
13 (MC35)
Ki* 17.7

Figure 1 (continued)

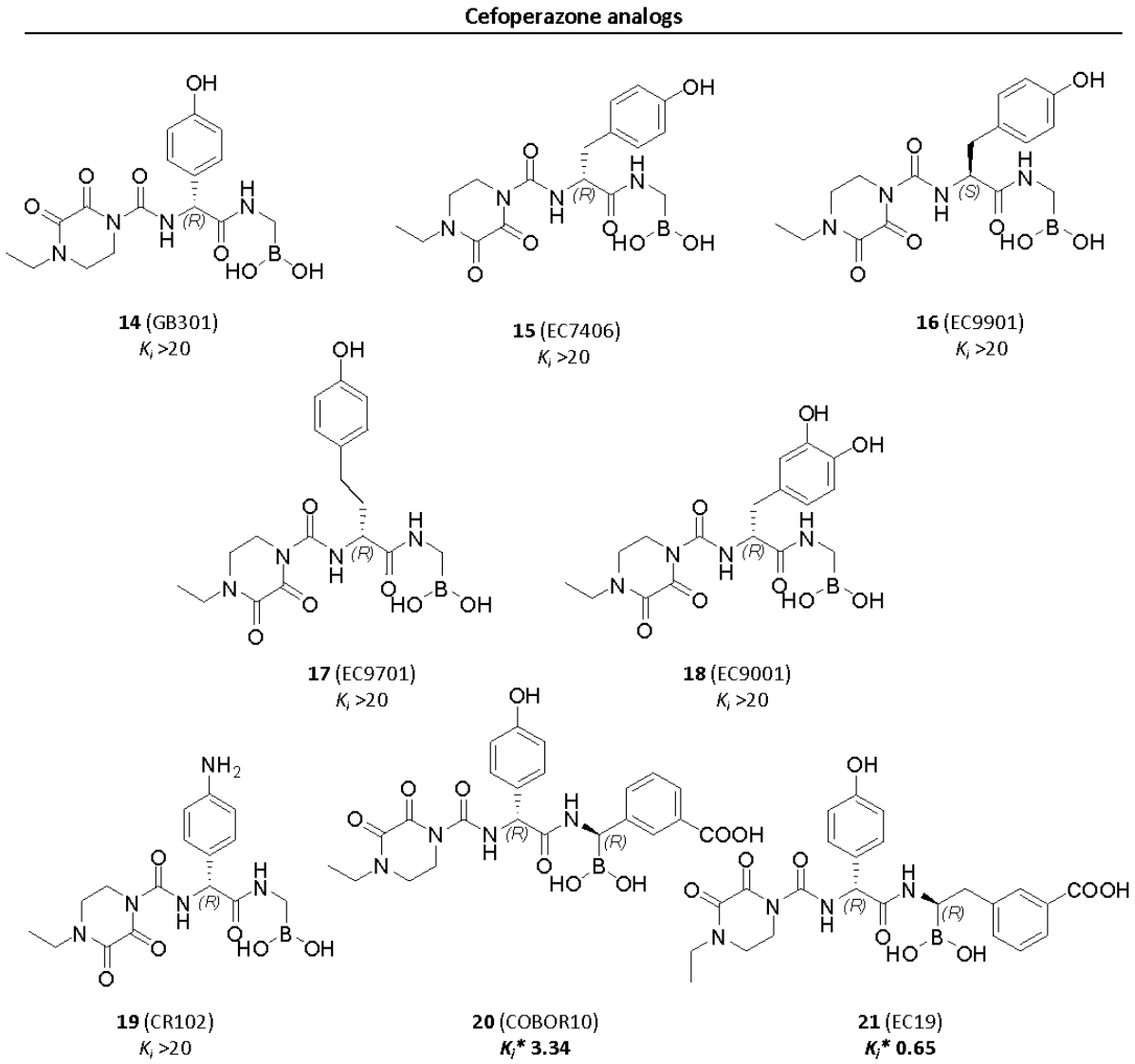

Figure 2

A

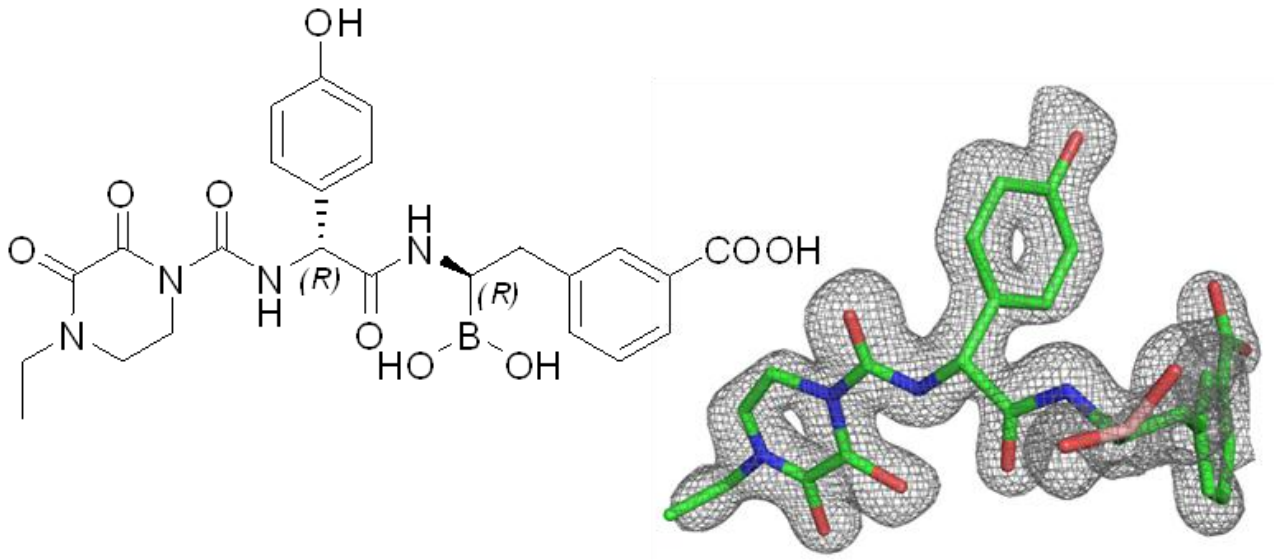
OH
O
O
N
N
H
(R)
O
N
H
(R)
O
HO
B
OH
COOH

B

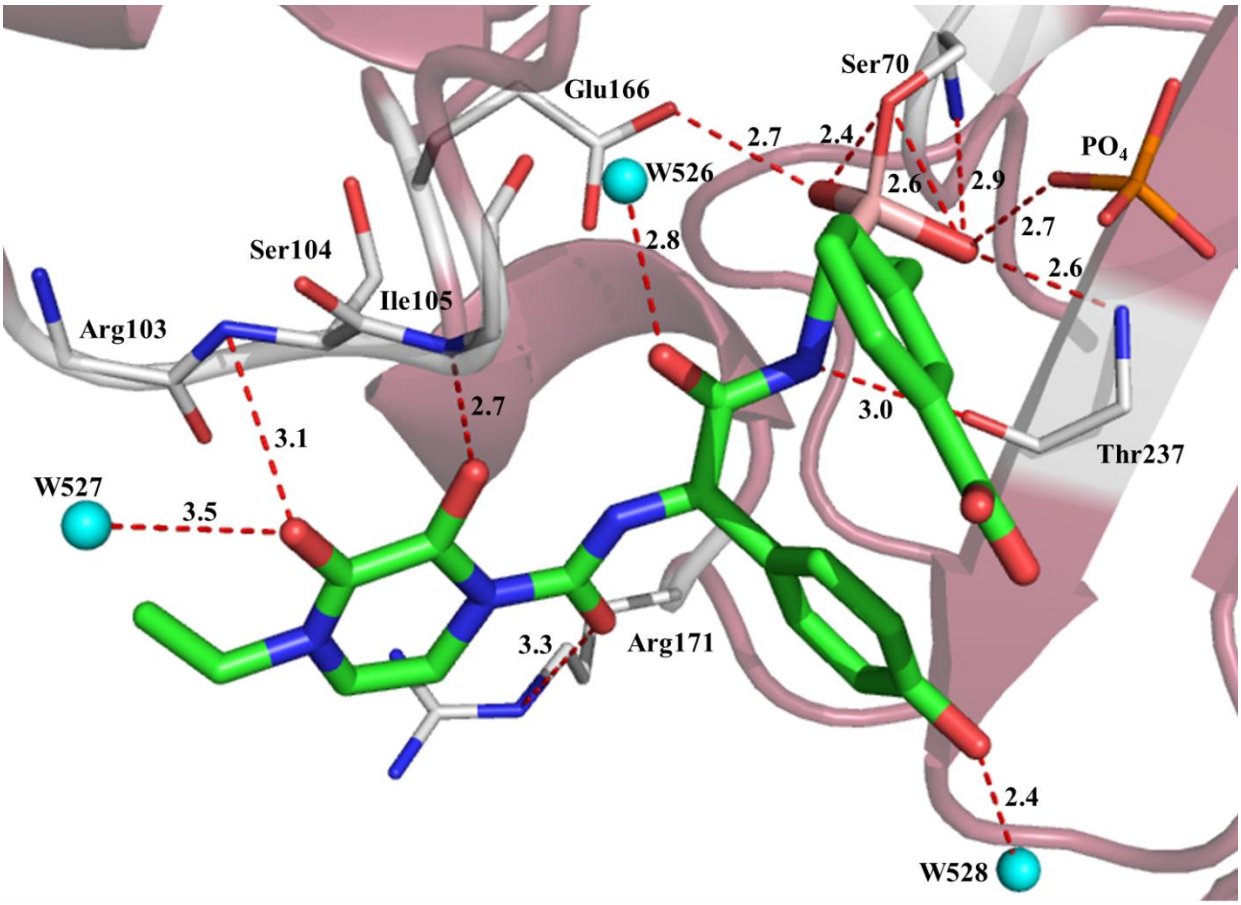
Glu166
Ser70
2.7
2.4
W526
2.6
2.9
PO4
2.7
2.8
2.6
Ser104
Ile105
Arg103
2.7
3.0
3.1
Thr237
W527
3.5
3.3
Arg171
2.4
W528

Figure 3